Metal-free Inorganic Ligands for Colloidal Nanocrystals: S^{2-}, HS^-, Se^{2-}, Te^{2-}, HTe^-, TeS_3^{2-}, OH^-, and NH^{2-} as Surface Ligands

Angshuman Nag, Maksym V. Kovalenko, Jong-Soo Lee, Wenyong Liu, Boris Sokoyny, and Dmitri V. Talapin*

1. Introduction

1.1. Colloidal Nanocrystals (NCs)

Colloidal semiconductor quantum dots (QDs): Electronic characteristics are closely related to the size (5~50 nm) and shape. (smaller size –> longer bandgap, quantum confinement effect)

Application: transistor, LED, diode laser, agents for medical imaging

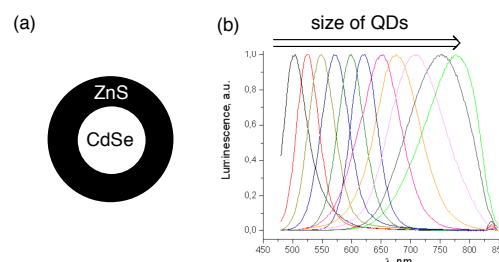**Drawback:** very low mobility (10^{-4} to 10^{-6} cm^2 V^{-1} s^{-1})

Figure 1. (a) A sketch of CdSe/ZnS core/shell NCs and (b) FL spectra of CdTe QDs of various sizes.

1.2. Design of Surface Ligands

Table 1. Different types of surface ligands used in nanocrystals and nanocrystal solids.

Ligand type	Molecular structure	Interparticle spacing	Functions, characteristics, typical examples
Molecules with single head group and a long hydrocarbon chain	C_n-tail, n=8–18 [1–3] ■ = HS-, COOH-, H$_2$N-, (OH)$_2$P(O)-, OP, N etc.	>1.5 nm	• Most common ligands used for NC synthesis • Formation of highly insulating NC solids • **PL quantum efficiency (QE) ~13%** • **µ of TOP/TOPO-cappped CdSe NCs not detected** (TOP/TOPO: trioctylphosphine/ trioctylphosphine oxide), **very low conductivity σ ~10^{-12}-10^{-9} S cm^{-1}**
Short-chain molecules with single head group	C_n-tail, n=2–8 ■ = HS-, COOH-, H$_2$N-	0.3–1 nm	• Treatment of NC solids or ligand-exchange in solutions • Decreased colloidal stability • Improved electronic transport compared to long-chain ligands • **Conductivities of up to 10^{-1} S cm^{-1} in arrays of metallic NCs**
Metal chalcogenide complexes	(Sn$_2$S$_6$ structure)	≥ 0.5 nm	• Prepared via solution phase ligand-exchange • Complete removal of original organic ligands • **3.3% QE** • **µ$_{sat}$ = 0.03 cm^2 V^{-1} s^{-1}, I_{ON}/I_{OFF} ~ 10^5** • **High conductivities of ~200 S cm^{-1} in Au-Sn$_2$S$_6$$^{4-}$ NC solids** • Switching the oxidation states in redox processes ex.) Sn$_2$S$_6$$^{2-}$: Sn^{4+} -> Sn^{2+}

1.3. This work: Metal-free Inorganic Ligands for Colloidal Nanocrystals

• The exchange of bulky organic surfactants with small inorganic ligands like S^{2-} or Se^{2-} should facilitate the electronic communication between individual NCs.

• Metal-free ligands allowed obtaining conductive NC layers without introducing foreign metal ions that often introduce recombination centers.
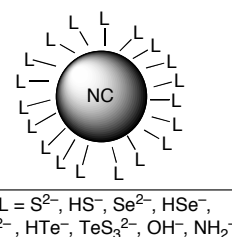

L = S^{2-}, HS^-, Se^{2-}, HSe^-, Te^{2-}, HTe^-, TeS_3^{2-}, OH^-, NH_2^-

Figure 2. A sketch of all-inorganic, metal-free ligand-capped colloidal nanocrystals.

2. Results and Discussion

2.1. Ligand Exchange

• The phase transfer can be easily monitored by the color change of toluene (red —> colorless) and formamide (FA) (colorless —> red) phases.

• Uncoordinated electrophilic Cd^{2+} sites —> Ligands exchange can be described as a nucleophilic substitution at the metal site.

2.2. Characterization

• The excitonic features in the absorption spectrum of 5.5 nm CdSe NCs remained unchanged after the ligand exchange: no changes in size, shape, and size-distribution of CdSe NCs (Figure 1a).

• CdSe with NCs with capped with S^{2-} ligands retained their band-edge PL—> S^{2-} ligands did not introduce midgap states serving as fast nonradiative recombination channels.

• <u>PL QE of S^{2-}-capped CdSe NCs which dropped to ca. 2% from ~13% of the NCs with organic ligands.</u>

• The transfer of NCs from toluene to FA resulted in complete disappearance of the bands at 2852 and 2925 cm^{-1} corresponding to C–H stretching in the original organic ligands (Figure 1b).

• Average hydrodynamic diameter of S^{2-}-capped NCs was smaller by ~1.7 nm than that of the same NCs capped with *n*-tetradecylphosphonic acid, which accounted for the effective length of the hydrocarbon chains (Figure 1c).

• The formation of stable colloidal solutions of negatively charged NCs in all cases of chalcogenide and hydrochalcogenide ligands (Figure 1d).

2.4. The hard and Soft Acids and Bases (HSAB) Classification applied to Colloidal Nanostructures

• Colloidal stabilization of NCs in FA was achieved through binding negatively charged ions to NC surface, leading to the formation of an electrical double layer around each NC. (Repulsive forces between NCs

Scheme 1. Ligand exchange with chalcogenide (S^{2-}, Se^{2-}, Te^{2-}), hydro-chalcogenide (HS^-, HSe^-, HTe^-) ions, TeS_3^{2-}, OH^-, NH_2^-.
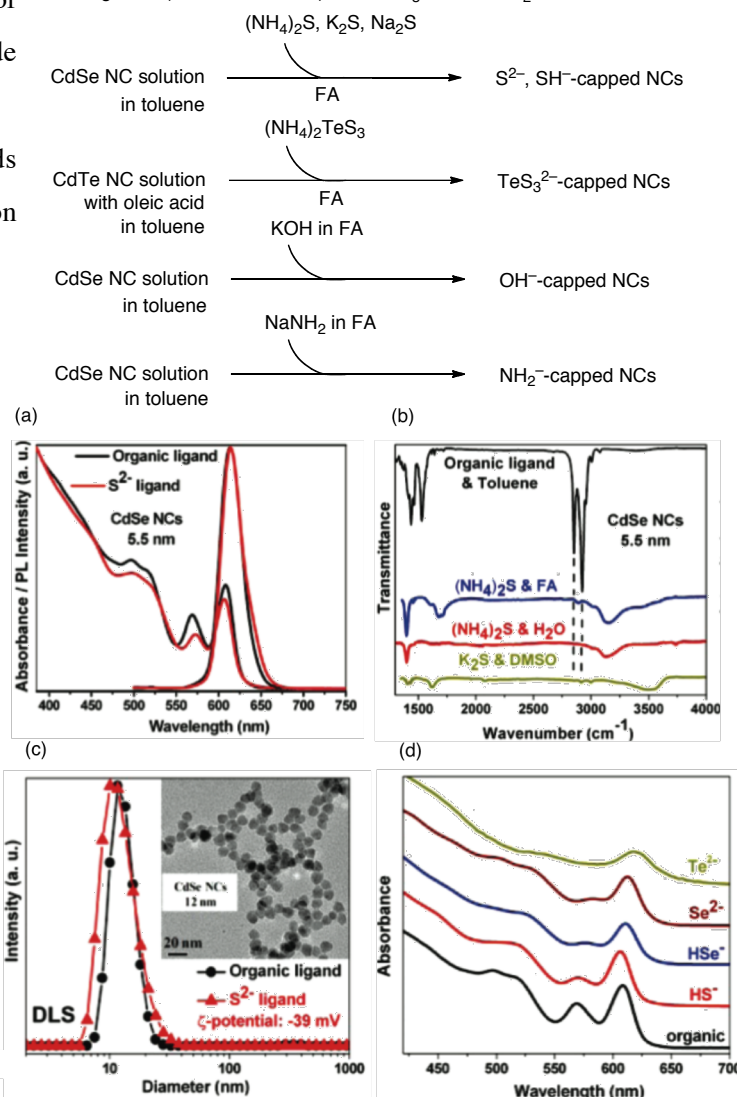

Figure 3. (a) Absorption and PL spectra of 5.5 nm CdSe NCs capped with organic ligands with organic ligands and S^{2-} ligand dispersed in toluene and FA, respectively. (b) FTIR spectra of 5.5 nm CdSe NCs with different combinations of ligands and solvents. (c) NC-size distributions measured by DLS for ~12 nm CdSe NCs capped with organic ligands and S^{2-} ions. Inset shows TEM image of the NCs capped with S^{2-} ligand. (d) Absorption spectra of 5.5 nm CdSe NCs capped with different ligands.
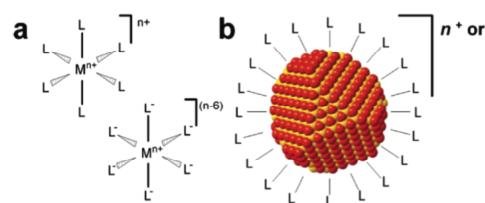
Scheme 2. (a) Typical metal complexes and (b) a n… crystal with surface ligands

prevent their aggregation.)

• In agreement with HSAB, soft Au^0 and Cd^{2+} sites exhibited stronger affinity to soft S^{2-} and HS^- ligands compared to hard OH^-, where harder Zn^{2+} sites in ZnSe and ZnO NCs had higher affinity to OH^- rather than to SH^- (Table 2).

• On the other hand, the extention of HSAB principle to NCs failed for InP and InAs NCs.

—> Free In^{3+} is a hard acid, while InAs and InP behave as soft acids preferentially binding to S^{2-} and HS^- rather than to OH^-.

—> Small difference in electronegativity between In and P or As let to reduced positive effective charge on the In sites which softens the acidic sites at InP and InAs NCs surface.

Table 2. Comparison of ζ-potential values for NCs capped with inorganic ligands.

NCs	Surface ligands (ζ-potential)	Do not provide colloidal stabilization
CdSe	S^{2-} (–40 mV), SH^- (–42 mV), OH^- (–20 mV)	
ZnSe	OH^- (–26 mV)	S^{2-}, SH^-
Au	S^{2-} (-60 mV), SH^- (–56 mV)	OH^-
InP	S^{2-} (–60 mV)	OH^-
InAs	S^{2-} (-39 mV), SH^- (–43 mV)	OH^-
In_2O_3	S^{2-} (–45 mV), SH^- (–40 mV), OH^- (–44 mV)	OH^-

• HSAB-based generalization of ligand exchange reactions is very useful for predicting the binding affinity between a given ligand and a given NC.

2.5. Ligand-Free Nanocrystals

• All-inorganic positively charged NCs are rare, because NCs typically have electrophilic metal-rich surfaces.

• To cleave the bonds between CdSe NC and carboxylate organic ligands without oxidizing the NC, HBF_4 and HPF_6 in polar solvent were used (Figure 4a).

• The size, size-distribution, and band-edge emission remained with a significant drop in the PL efficiency (< 0.5 % for CdSe NCs and ~2 % for CdSe/ZnS NCs).

• ζ-potentials of CdSe and CdSe/ZnS NCs were measured to be around +30 mV, sufficient for electrostatic stabilization of the colloidal dispersion.

• The absence of C–H bands at 2852 and 2925 cm^{-1} —> complete removal of the original organic ligand (Figure 4b).
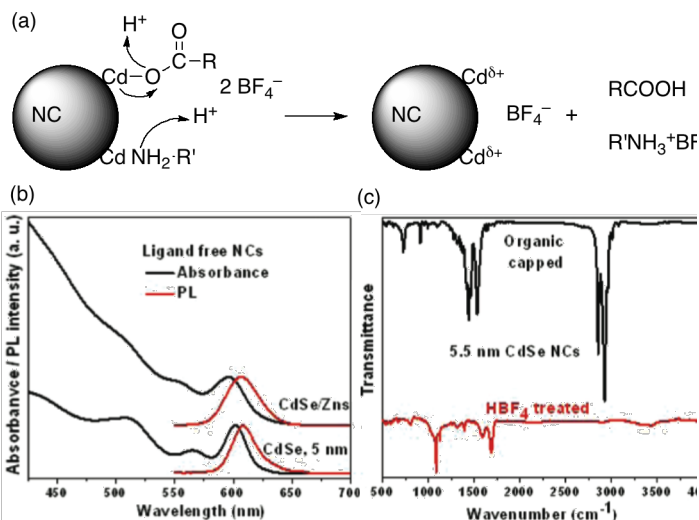

Figure 4. (a) Removal of the organic ligands from the surface of CdSe NC by HBF_4 treatment. (b) Absorption and PL spectra of ligand-free colloidal CdSe and CdSe/ZnS NCs obtained after HBF_4 treatment. (c) FTIR spectra of originally capped and ligand-free CdSe NCs after HBF_4 treatment.

2.6. Colloidal NCs with Metal-Free Inorganic Ligands for FET

• The NC films were spin-coated from FA solutions at 80 ˚C to improve the contact, followed by short annealing at 200–250 ˚C to remove solvents and remaining volatile ligands.

Figure 5 shows sets of drain current (I_D) versus drain-source voltage (V_{DS}) scans at different gate voltages (V_G) for devices made of $(NH_4)_2S^-$ capped 4.6 nm CdSe NCs, 10 nm CdSe/CdS, and 8 nm CdSe/ZnS core/shell NCs.
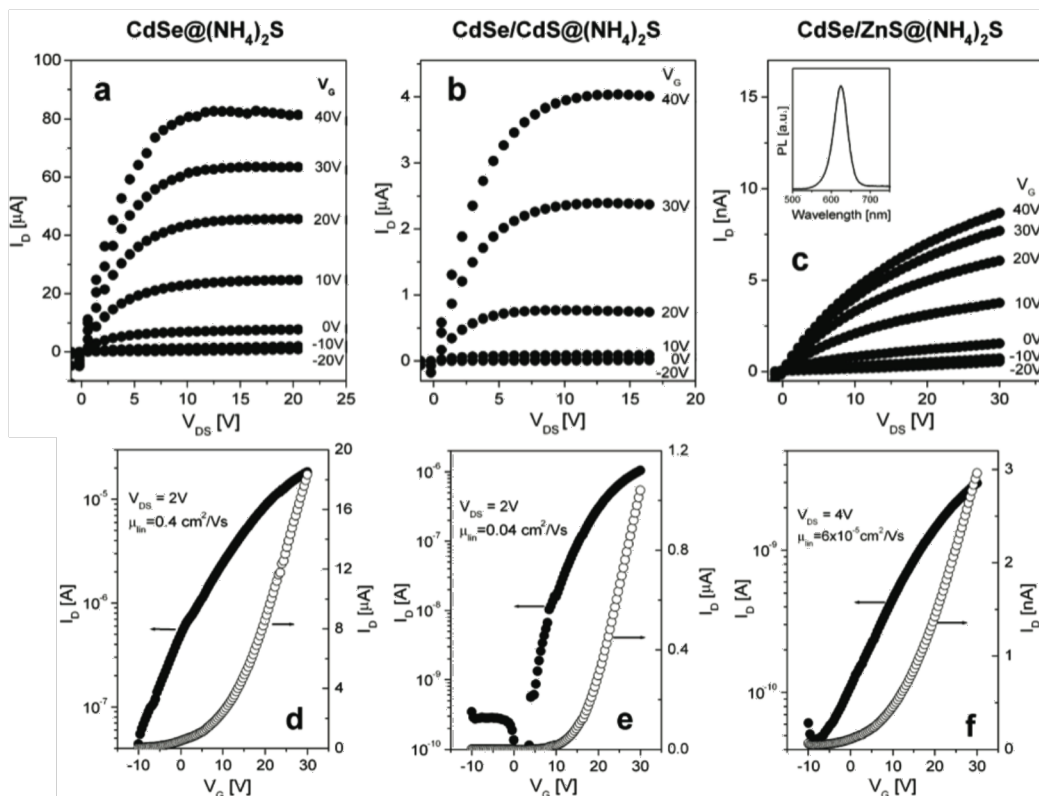
3

Figure 5. (a–c) Plots of drain current I_D versus drain-source voltage V_{DS}, measured at different gate voltages V_G for the field-effect transistor (FETs) assembled from colloidal NCs capped with $(NH_4)_2S$. (d–f) Plots of I_D vs V_G at constant V_{DS} = 2, 4 V used to calculate current modulation and linear regime field-effect mobility for FETs. Channel length: $L = 80\ \mu$m, $W = 1500\ \mu$m, 100 nm SiO_2.

Table 3. Electron mobilities corresponding to the linear regime of FET operation.

	Annealing temperature (˚C)	V_{DS} (V)	μ_{lin} (cm² V⁻¹ s⁻¹)	I_{ON}/I_{OFF}
CdSe NCs capped with $(NH_4)_2S$	200	2	0.4	~10^3
CdSe/CdS core–shell NCs capped with $(NH_4)_2S$	250	2	0.04	~10^4
CdSe/ZnS core–shell NCs capped with $(NH_4)_2S$	250	4	6×10^{-5}	~10^2

• With increasing V_G, I_D increased characteristic of the n-type transport (Figure 5d, 5e, 5f).

• Although the films of CdSe/ZnS core–shell NCs showed rather low carrier mobility, these NCs preserved bright bandage PL even after annealing at 250 ˚C (insets in Figure 5c).

3. Summary

• Various metal-free inorganic ligands behave as capping ligands for colloidal semiconductor and metallic NCs.

• The use of small inorganic ligands instead of traditional ligands with long hydrocarbon tails **facilitated the charge transport** between nanocrystals, even though **the significant drop of QE** was observed.

4. References

1. Talapin, D. V.; Lee, J.; Kovalenko, M. V.; Schevchenko, E. V. *Chem. Rev.* **2010**, *110*, 389–458.

2. Dong, C.; Ye, X.; Chen, J.; Kang, Y.; Gordon, T.; Kikkawa, J. M.; Murray, C. B. *J. Am. Chem. Soc.* **2011**, *133*, 998–1006.